J Therm Anal Calorim (2009) 97:929–935
DOI 10.1007/s10973-009-0121-5

Thermal degradation of poly(lactic acid) measured by thermogravimetry coupled to Fourier transform infrared spectroscopy

Hantao Zou · Changhai Yi · Luoxin Wang · Hongtao Liu · Weilin Xu

Received: 21 October 2008 / Accepted: 3 March 2009 / Published online: 19 June 2009

Abstract Thermal decomposition of poly(lactic acid) (PLA) has been studied using thermogravimetry coupled to Fourier transform infrared spectroscopy (TGA-FTIR). FTIR analysis of the evolved decomposition products shows the release of lactide molecule, acetaldehyde, carbon monoxide and carbon dioxide. Acetaldehyde and carbon dioxide exist until the end of the experiments, whereas carbon monoxide gradually decreases above the peak temperature in that the higher temperature benefits from chain homolysis and the production of carbon dioxide. A kinetic study of thermal degradation of PLA in nitrogen has been studied by means of thermogravimetry. It is found that the thermal degradation kinetics of PLA can be interpreted in terms of multi-step degradation mechanisms. The activation energies obtained by Ozawa–Flynn–Wall method and Friedman's method are in good agreement with that obtained by Kissinger's method. The activation energies of PLA calculated by the three methods are 177.5 kJ mol^{-1}, 183.6 kJ mol^{-1} and 181.1 kJ mol^{-1}, respectively.

Keywords Poly(lactic acid) (PLA) · FTIR · TGA · Activation energy · Thermal degradation kinetics

H. Zou (✉) · C. Yi · L. Wang · H. Liu · W. Xu
Key Laboratory of Green Processing and Functional Textile of New Textile Materials, Ministry of Education, Wuhan University of Science and Engineering, Wuhan, Hubei 430073, People's Republic of China
e-mail: zouhantao@mail.dhu.edu.cn

Introduction

Poly(lactic acid) (PLA) has received more attention due to renewable resources, biocompatibility, biodegradability, mechanical property, thermoplastic processibility et al. [1, 2]. Therefore it has received much interest for its medical, pharmaceutical, packing, clothing and environmental applications [2–4].

But PLA belongs to the group of polymers with poor thermal stability and is highly sensitive to heat, which influences the processing and spinning of PLA [5]. So lots of studies on the thermal degradation and thermal stability of PLA have been reported. McNeill and Leiper investigated the degradation of poly(L-lactic acid) (PLLA) under both controlled heating conditions and isothermal conditions by thermal volatilization analysis [6, 7]. In their research they employed a 1st-order reaction kinetic equation to calculate the apparent activation energy E to be 119 kJ mol^{-1} in the range of 240–270 °C. Kopinke and co-workers reported a multi step process for PLLA pyrolysis. They found that intra-molecular transesterification was a dominant degradation pathway, and the pyrolysis behavior was different between pure and Sn-containing PLLAs [8, 9]. Cam and Marucci also reported that some metal compounds, such as Sn, Zn, Al and Fe, had a great influence on the pyrolysis behavior of PLLA [10]. Babanalbandi et al. reported E values for PLLA pyrolysis using isothermal methods [11]. Their results showed that at first the E value decreased from 103 to 72 kJ mol^{-1} with increasing weight loss and then enhanced up to a value of 97 kJ mol^{-1}. They postulated that the PLLA degradation process followed more complex kinetics, even at low conversion. Aoyagi et al. studied the degradation behavior of PLLA, and found that the E values changed in the range of 80–160 kJ mol^{-1} with the change in weight

loss, and concluded that the pyrolysis of PLLA involved more than two mechanisms [12]. Fan investigated the thermal stability of PLA with carboxyl and calcium salt end [13] and acetyl group end [14]. They reported that the E value was related to the residual catalyst metal, for a highly purified PLLA the E was 176 kJ mol^{-1}; for a PLLA with Sn content of 437 ppm the E value was relatively constant at 128–130 kJ mol^{-1} during the whole pyrolysis. They clarified that various degradation processes occurred each having individual kinetic parameters, which depended on the PLLA's Sn content and end structure, as well as the temperature of pyrolysis. They attributed the reasons to various types of degradation mechanisms dependent on the Sn content and end structure [13–15]. Nishida et al. [16] also reported the effect of tin on PLLA pyrolysis. The dynamic pyrolysis of PLLA-Sn sample by TG clearly indicated that with an increase in Sn content there was a shift to a lower degradation range and a decrease in activation energy E. Liu and co-workers reported the kinetics of thermo-oxidative and thermal degradation of poly(D,L-lactic acid) (PDLLA) at processing temperature. Results showed that there were two to three stages [17]. The 1st stage was dominated by the oligomers containing carboxylic acid groups and hydroxyl groups, during which oxygen and nitrogen had little effect on the degradation, thus they share similar E. When the oligomers were consumed over or evaporated, the 2nd stage began, and oxygen had a promoting effect on the thermo-oxidation process, resulting in the great decrease in E. The third stage of PDLLA was observed when it degraded under nitrogen over 200 °C, which was caused by the appearance of carboxylic acid substance.

This report focuses on such an investigation of the thermal degradation of poly(lactic acid) in nitrogen using thermal analysis-Fourier transform infrared spectroscopy (TG-FTIR). The gaseous decomposition products of PLA at different temperatures are confirmed. The thermal degradation kinetics of PLA in nitrogen is investigated by thermogravimetry. The Ozawa–Flynn–Wall method, Friedman's method and Kissinger's method are used to calculate the activation energy of PLA.

Experimental

Sample

PLA was kindly supplied by Dikang Zhongke Co. Ltd. (China). The intrinsic viscosity values $[\eta]$of PLA was measured with an Ubbelohde viscosimeter in tetrahydrofuran chloroform at 31 °C, and the molecular weight (69,000) of PLA was estimated from equation:$[\eta] = 5.50\times 10^{-4} \times M^{0.639}$[17].

Measurements

Thermal analysis-Fourier transform infrared spectroscopy

Thermal analysis-Fourier transform infrared spectroscopy (TGA-FTIR) was carried out at a heating rate of 20 °C min^{-1} on a TG 209 instrument (NETZSCH, Germany) which was connected to Tensor 27 FTIR (Bruker, Germany) through stainless steel tubing. Dry nitrogen gas with a flow of 60 mL/min carried the decomposition products through steel tubing into the gas cell for IR detection. Both the transfer line and the gas cell were kept at 250 °C to prevent gas condensation. IR spectra were recorded in the spectral range of 4000–650 cm^{-1} with a 4 cm^{-1} resolution and averaging 8 scans.

Thermogravimetric analysis

The thermogravimetric analysis (TGA) was performed with a TG 209 instrument (NETZSCH, Germany). Samples (10 ± 0.1 mg) were placed on an open Al_2O_3 pan, and the experiments conducted in N_2 at a flow rate of 20 mL min^{-1}. The heating rates of 5, 10, 20, 30, 40 °C min^{-1} were used and continuous records of sample temperature, sample weight, and its first derivative were taken.

Kinetic methods

Ozawa–Flynn–Wall method

Activation energy E can be calculated by various methods. The first method, the isoconversional method of Ozawa–Flynn–Wall (OFW) [18, 19] is, in fact, a "model free" method which assumes that the conversion function $f(\alpha)$ does not change with the alteration of the heating rate for all values of the conversion degree α. It involves the measuring of the temperatures corresponding to fixed values of α from experiments at different heating rates β. Therefore, plotting ln (β) against $1/T$ should give straight lines and its slope is directly proportional to the activation energy ($-E/R$). The equation is the following form:

$$\ln \beta = \ln \frac{AE}{R} - \ln F(\alpha) - \frac{E}{RT} \quad (1)$$

where T is the absolute temperature, β is the heating rate, E is the activation energy, A is the pre-exponential factor (min^{-1}), α is the conversion degree and R is the universal gas constant (8.314 J/K mol).

If the determined activation energy is the same for the various values of α, the existence of a single-step reaction can be concluded with certainty. On the contrary, a change of E with increasing degree of conversion is an indication

of a complex reaction mechanism that invalidates the separation of variables involved in the Ozawa–Flynn–Wall analysis [20, 21]. The Ozawa–Flynn–Wall method is the most useful method for the kinetic interpretation of the thermogravimetric data obtained when studying complex processes, like the thermal degradation of polymers. This method can determine the activation energy without a knowledge of reaction order [22].

Friedman's method

Friedman [23] proposed the use of the logarithm of the conversion rate $d\alpha/dT$ as a function of the reciprocal temperature, in the form of

$$\ln\left(\frac{d\alpha}{dT}\right) = \ln\left(\frac{A}{\beta}\right) + \ln(f(\alpha)) - \frac{E}{RT} \quad (2)$$

It is obvious from Eq. 2 that if the function $f(\alpha)$ is constant for a particular value of α, then the sum $\ln(f(\alpha)) + \ln(A/\beta)$ is also constant. It is easy to obtain the E values over a wide range of conversions by plotting $\ln(d\alpha/dT)$ against $1/T$ at constant values of α. The slopes $(-E/R)$ of these straight lines are directly proportional to the reaction activation energy E.

Kissinger's method

The third one is based on Kissinger's method [24, 25] that has been used in the literature to determine the activation energy from plots of the logarithm of the heating rate versus the inverse of the temperature at the maximum reaction rate in constant heating rate experiments.

The activation energy can be determined by the Kissinger's method without a precise knowledge of the reaction mechanism [24], using the following equation:

$$\ln\left(\frac{\beta}{T_p^2}\right) = \ln\frac{AR}{E} + \ln\left[n(1-\alpha_p)^{n-1}\right] - \frac{E}{RT_p} \quad (3)$$

where T_p and α_p are the absolute temperature and the conversion at the maximum weight-loss rate, n is the reaction order, A, β and E have the above meanings.

From the plots of $\ln\left(\beta/T_p^2\right)$ versus $1/T_p$ and fitting to a straight line, the activation energy E can be calculated from the slope.

Results and discussion

Thermal stability

The thermogravimetric (TG) and derivative thermogravimetric (DTG) curves of PLA at different heating rates: 5, 10, 20, 30 and 40 °C min^{-1} are shown in Fig. 1. The TG

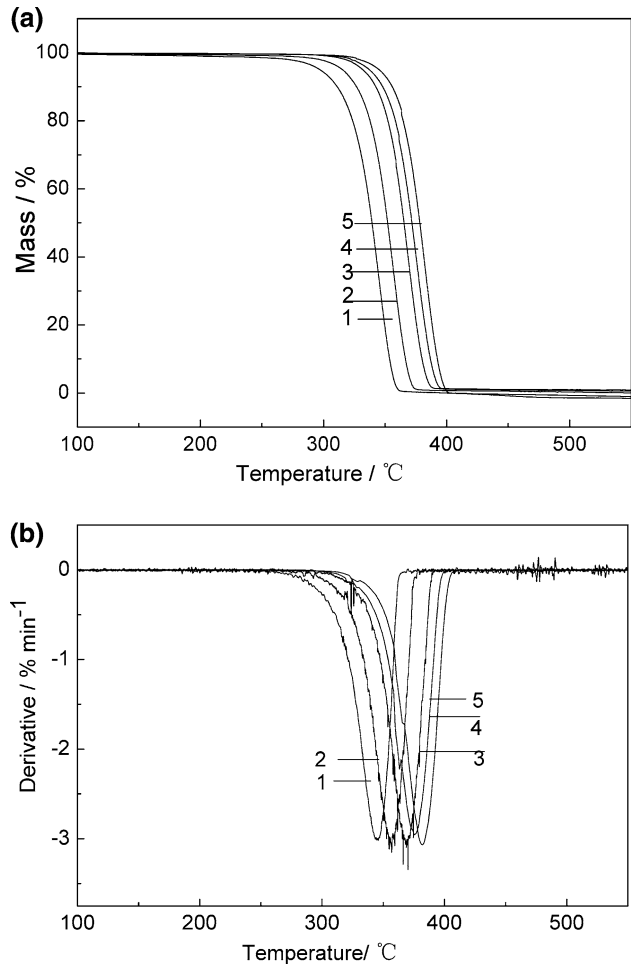

Fig. 1 **a** The TG curves and **b** DTG curves of PLA at different heating rates β (1) 5 °C min^{-1} (2) 10 °C min^{-1} (3) 20 °C min^{-1} (4) 30 °C min^{-1} (5) 40 °C min^{-1}

characteristic temperatures of PLA at the different heating rates are illustrated in Table 1. The TG curves shift to higher temperature as the heating rate β increases from 5 °C min^{-1} to 40 °C min^{-1}. At ≈275 °C PLA begins to decompose and completes the decomposition at ≈420 °C. The shift of onset to higher temperature with increasing β is due to the shorter time required for a sample to reach a

Table 1 Characteristic temperatures of thermal degradation of PLA

β (°C min^{-1})	T_i (°C)	T_p (°C)	T_d of 5% loss (°C)	T_d of 10% loss (°C)
5	322.4	348.3	297.1	311.2
10	335.5	359.6	315.4	326.9
20	346.0	370.2	332.0	342.5
30	354.5	377.0	337.3	348.1
40	361.7	381.3	345.2	355.8

T_i: Onset temperature of TG; T_p: Peak temperature of DTG; T_d: Decomposition temperature at a settled temperature

given temperature at the faster heating rates. This heating-rate dependence is also indicated in the DTG curves. That is, the peaks of the DTG curves shift towards higher temperatures as the heating rate increases.

The gaseous products of the decomposition process

In order to obtain information about the evolution with the temperature of the composition of the gas evolved from the TGA furnace, the three-dimensional diagrams (3D diagrams) corresponding to the thermal degradation of PLA has been obtained in Fig. 2. The *X* axis, *Y* axis and *Z* axis represent the wavenumber (cm^{-1}), absorbance units and time of the process, respectively. It is shown that the volatile products of thermal decomposition of PLA are released with the highest intensity at 1060 s, which corresponds to the time at the peak temperature of DTG diagram, that is 1052 s. Therefore the lag time from furnace of TGA to gas cell of FTIR is 8 s. And then a gradual decrease of the described intensity of absorption bands could be observed after the highest intensity. The main decomposition process is completed at 800–1200 s corresponding to 282–418 °C of TGA at the heating rate of 20 °C min^{-1}.

Figures 3 and 4 show the FTIR spectra of gaseous products evolved at different temperatures and at the peak temperature (370.2 °C) of 20 °C min^{-1}, respectively. In Figs. 3 and 4, two remarkable absorption peaks at 1750 cm^{-1} and 2747 cm^{-1} can be observed until the end of the experiments. The two peaks are corresponding to the C=O band stretching vibration [26] and the aldehydic C–H stretching vibration [27], respectively. Combined with the peaks at 3010 and 2930 cm^{-1} of C–H stretching vibration and at 1445 and 1380 cm^{-1} of C–H bending vibration of CH_3 [6], it demonstrates that aldehyde is formed during the degradation of PLA.

Correspondingly, FTIR spectra show absorption bands attributed to C–O stretching (at 1260 and 1100 cm^{-1}) [7],

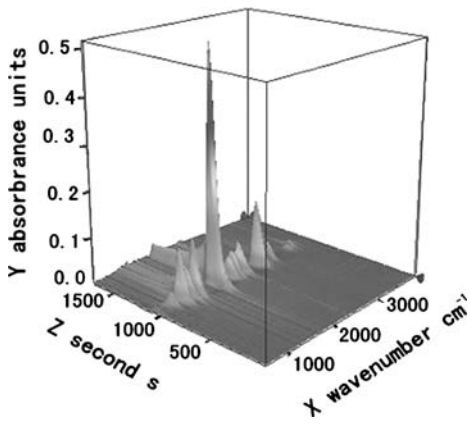

Fig. 2 3D-FTIR spectra of the evolved gaseous products at 20 °C min^{-1}

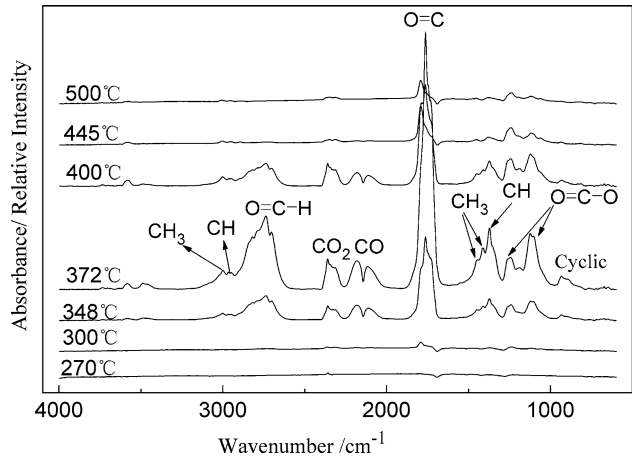

Fig. 3 FTIR of gaseous products evolved at different temperatures

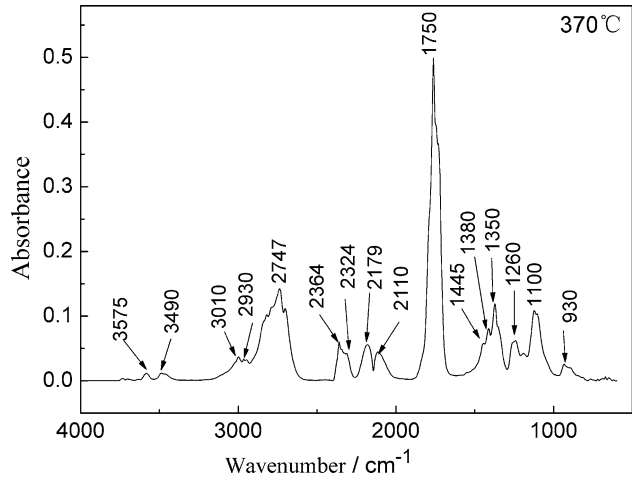

Fig. 4 FTIR of gaseous products evolved at 372 °C

C=O stretching (at 1750 cm^{-1}) of carbonyl group [26], C–H stretching and bending (at 2930 and 1380 cm^{-1}) of methyl groups [17], and a ring skeletal vibration (at 930 cm^{-1}). It implies that the evolved products include lactide or cyclic oligomer both by ester interchange and by chain homolysis route of PLA, which is presented by McNeil and Leiper using thermal volatilization analysis [6].

Carbon dioxide (CO_2) is identified by the presence of two bands located at 2364 and 2324 cm^{-1} according to the previous reports [28, 29]. Therefore, CO_2 is one of the main decomposition products, which is attributed to the thermal degradation based upon chain homolysis of PLA [6]. It can be observed from 300 °C until the end of the experiment from the FTIR spectra. Carbon monoxide (CO) is found to be present from the peaks at 2179 and 2110 cm^{-1} assigned to C–O bending vibration [30]. The formation of carbon monoxide is attributed to the decomposition dependent upon a hydroxyl end-initiated ester.

But, it is noteworthy that the intensity of the peak of CO decreases more obviously than that of CO_2 over the peak temperature, which is agreement with the mechanism that somewhat higher temperature benefits from chain homolysis which gives the product of CO_2 [6]. In addition, the peaks over 3500 cm^{-1} are attributed to water in FTIR spectra.

Thermal degradation kinetics

Ozawa–Flynn–Wall method

Firstly, the isoconversional Ozawa–Flynn–Wall (OFW) method, Eq. 1, is used to calculate the activation energy of PLA for different conversion values from a linear fitting of ln β versus 1/T. For this study, the conversion values are 0.20, 0.30, 0.40, 0.50, 0.60, 0.70, 0.80, 0.90. The Ozawa–Flynn–Wall plots for PLA with correlation coefficient greater than 0.99 are shown in Fig. 5 and the activation energies are summarized in Table 2. It shows that the fitting straight lines are nearly parallel, which implies that this method is applicable to PLA in the conversion range studied. In Table 2, a change of E with increasing degree of conversion is an indication of a complex decomposition mechanism of PLA [20, 21, 31].From the activation energies calculated from the slopes corresponding to the different conversions, a mean value of 177.5 kJ mol^{-1} is found, which is agreement with the activation energy reported in the reference [13].

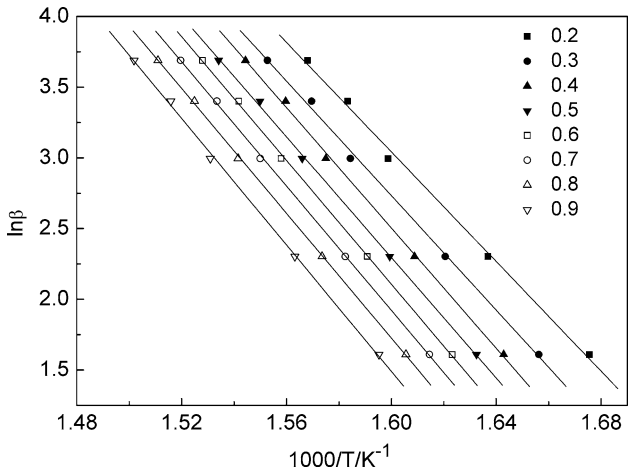

Fig. 5 Ozawa–Flynn–Wall plots of PLA at different conversions

Friedman's method

Friedman's method is used Eq. 2 by plotting $\ln(d\alpha/dT)$ against 1/T for a constant α value and the activation energy is calculated and shown also in Table 2. Obviously, the E values calculated by Friedman's method are slightly larger than those of Ozawa–Flynn–Wall method. The difference in the E value calculated by the two methods can be explained as follows. It is well known that Friedman's method is very sensitive to experimental noise, and tends to be numerically unstable because of employing instantaneous rate value [32]. On the other hand, the Ozawa–Flynn–Wall method produces a systematic error in E when the activation energy varies with conversion [33]. However, both methods reveal the same trend of activation energies for the whole conversion range studied, that is, the E values calculated by the each method increase with increasing the conversion degree. The increase of E value with conversion means that the observed kinetics can only be interpreted in terms of multi-step degradation mechanisms [31], which is consistent with the reports in the references [11, 12, 17]. The mean value of E calculated by Friedman's method is 183.6 kJ mol^{-1}.

Kissinger's method

Using Eq. 3 and the inflection point temperatures corresponding to the thermograms shown in Fig. 6, the activation energy can be calculated by the slope of the linear

Table 2 Activation energies of PLA using Ozawa–Flynn–Wall and Friedman's methods

Conversion α	Ozawa–Flynn–Wall method		Friedman's method	
	E (kJ mol^{-1})	Correlation coefficient (r)	E (kJ mol^{-1})	Correlation coefficient (r)
0.2	161.1	0.9985	171.9	0.9995
0.3	168.4	0.9989	173.4	0.9965
0.4	176.9	0.9993	175.6	0.9995
0.5	177.3	0.9996	181.2	0.9954
0.6	182.0	0.9997	185.4	0.9987
0.7	182.7	0.9998	190.9	0.9985
0.8	183.5	0.9998	193.9	0.9870
0.9	188.0	0.9995	196.5	0.9895
Average	177.5		183.6	

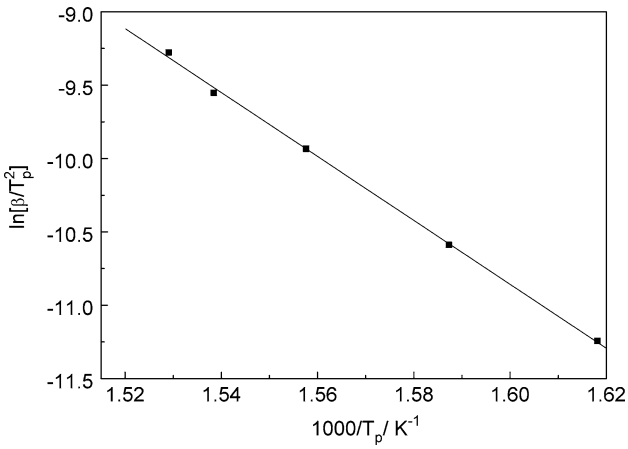

Fig. 6 Kissinger curve of $\ln\left(\beta/T_p^2\right)$ versus $1/T_p$ of PLA

relationship $\ln\left(\beta/T_p^2\right)$ versus $1/T_p$. The E value (181.1 kJ mol^{-1}) is obtained from Kissinger's curve with correlation coefficient greater than 0.9977. Moreover, it is found that the value of E (181.1 kJ mol^{-1}) calculated by Kissinger's method coincides with those calculated using the above two methods.

Conclusions

Thermogravimetry coupled to Fourier transform infrared spectroscopy (TGA-FTIR) has been used to study the thermal decomposition products evolved during the degradation of poly (lactic acid) (PLA) in nitrogen at a heating rate of 20 °C min^{-1}. The gaseous products of cyclic oligomers, lactide, acetaldehyde, carbon monoxide and carbon dioxide are observed, which is attributed to the thermal degradation of PLA based upon a hydroxyl end-initiated ester interchange process and chain homolysis. Acetaldehyde and carbon dioxide exist in the products until the end of the experiments, whereas carbon monoxide gradually decreases above the peak temperature in that the higher temperature benefits from chain homolysis. Thermal decomposition of PLA has been studied using thermogravimetry. The TG thermograms shift to higher temperature as the heating rate increases from 5 °C min^{-1} to 40 °C min^{-1}. The thermal degradation kinetics of PLA can be interpreted in terms of multi-step degradation mechanisms. At last, the activation energies of PLA determined by Ozawa–Flynn–Wall method, Friedman's method and Kissinger's method are consistent and 177.5 kJ mol^{-1}, 183.6 kJ mol^{-1} and 181.1 kJ mol^{-1}, respectively.

Acknowledgements The financial support of the Scientific Research Foundation of Hubei Provincial Education Department (No: B200717003) and the Research Foundation of Wuhan University of Science and Engineering in China (No. 20073202) is greatly acknowledged.

References

1. Chow WS, Lok SK. Thermal properties of polylactides effect of molecular mass and nature of lactide isomer. J Therm Anal Calorim. 2009;95:957–64.
2. Ahmed J, Zhang JX, Song Z, Varshney SK. Thermal properties of poly(lactic acid)/organo-montmorillonite nanocomposities. J Therm Anal Calorim. 2009;95:627–32.
3. Drumond WS, Mothé CG, Wang SH. Quantitative analysis of biodegradable amphiphilic poly(*L*-lactide)-block-poly(ethyleneglycol)-blockpoly(*L*-lactide) by using TG, FTIR and NMR. J Therm Anal Calorim. 2006;85:173–7.
4. Martino VP, Ruseckaite RA, Jiménez A. Thermal and mechanical characterization of plasticized poly (*L*-lactide-co-*D*,*L*-lactide) films for food packaging. J Therm Anal Calorim. 2006;86:707–12.
5. Jamshidi K, Hyon SH, Ikada Y. Thermal characterizaton of polylactides. Polymer. 1988;29:2229–34
6. McNeill IC, Leiper HA. Degradation studies of some polyesters and polycarbonates-2. Polylactide: degradation under isothermal conditions, thermal degradation mechanism and photolysis of the polymer. Polym Degrad Stab. 1985;11:309–26.
7. McNeill IC, Leiper HA. Degradation studies of some polyesters and polycarbonates-1. Polylactide: general features of the degradation under programmed heating conditions. Polym Degrad Stab. 1985;11:267–85.
8. Kopinke FD, Remmler M, Mackenzie K, Moder M. Thermal decomposition of biodegradable polyesters-II. Poly (lactic acid). Polym Degrad Stab. 1996;53:329-42.
9. Kopinke FD, Mackenzie K. Mechanism aspects of the thermal degradation of poly(lactic acid) and poly (b-hydroxybutyric acid). J Anal Appl Pyrol. 1997;40:43–53.
10. Cam D, Marucci M. Influence of residual monomers and metals on poly (L-lactide) thermal stability. Polymer. 1997;38:1879–84.
11. Babanalbandi A, Hill DJT, Hunter DS, Kettle L. Thermal stability of poly(lactic acid) before and after g-radiolysis. Polym Int. 1999;48:980–84.
12. Aoyagi Y, Yamashita K, Doi Y. Thermal degradation of poly[(*R*)-3-hydroxybutyrate], poly[ε-caprolactone], and poly[(*S*)-lactide]. Polym Degrad Stab. 2002;76:53–9.
13. Fan YJ, Nishidaa H, Shiraib Y. Pyrolysis kinetics of poly (L-lactide) with carboxyl and calcium salt end structures. Polym Degrad Stab. 2003;79:547–62.
14. Fan YJ, Nishidaa H, Shiraib Y. Thermal stability of poly (L-lactide): influence of end protection by acetyl group. Polym Degrad Stab. 2004;84:143–9.
15. Fan YJ, Nishidaa H, Shiraib Y. Thermal degradation behaviour of poly(lactic acid) stereocomplex. Polym Degrad Stab. 2004; 86:197–208.
16. Nishidaa H, Mori T, Hoshihara S. Effect of tin on poly(l-lactic acid) pyrolysis. Polym Degrad Stab. 2003;81:515–23.
17. Liu XB, Zou B, Li WT. Kinetics of thermo-oxidative and thermal degradation of poly(*D*,*L*-lactide) (PDLLA) at processing temperature. Polym Degrad Stab. 2006;91:3259–65.
18. Ozawa T. A new method of analyzing thermogravimetric data. Bull Chem Soc Jpn. 1965;38:1881–91.
19. Flynn JH, Wall LA. A quick, direct method for the determination of activation energy from thermogravimetric data. Polym Lett. 1966;4:323–8.
20. Chrissafis K, Paraskevopoulos KM, Bikiaris DN. Thermal degradation mechanism of poly(ethylene succinate) and poly(butylene succinate): comparative study. Thermochimica Acta. 2005;435:142–50.
21. Chrissafis K, Paraskevopoulos KM, Bikiaris DN. Thermal degradation kinetics of the biodegradable aliphatic polyester, poly(propylene succinate). Polym Degrad Stab. 2006;91:60–8.

22. Corneliu H, Tachita VB, Oana P. Kinetics of thermal degradation in non-isothermal conditions of some phosphorus-containing polyesters and polyesterimides. Eur Polym J. 2007;43:980–8.
23. Friedman HL. Kinetics of thermal degradation of char-forming plastics from thermogravimetry. Application to phenolic plastic. J Polym Sci Part C. 1964;6:183–95.
24. Kissinger HE. Variation of peak temperature with heating rate in differential thermal analysis. J Res Nat Bur Stand. 1956;57: 217–21.
25. Kissinger HE. Reaction kinetics in differential thermal analysis. Anal Chem. 1957;29:1702–12.
26. Jang BN, Wilkie CA. The thermal degradation of bisphenol A polycarbonate in air. Thermochimica Acta. 2005;426:73–84.
27. Marcilla A, Gomez-Siurana A, Menargues S. Qualitative study of the evolution of the composition of the gas evolved in the thermal and HY-catalytic oxidative degradation of EVA copolymers. Thermochimica Acta. 2005;438:155–63.
28. Xie W, Gao ZM, Pan WP. Thermal degradation chemistry of alkyl quaternary ammonium montmorillonite. Chem Mater. 2001;13:2979–90.
29. Xie W, Gao ZM, Liu KL. Thermal characterization of organically modified montmorillonite. Thermochimca Acta. 2001;367–368:339–50.
30. Wang GA, Cheng WM, Tu YL. Characterizations of a new flame-retardant polymer. Polym Degrad Stab. 2006;91:3344–53.
31. Vyazovkin S, Sbirrazzuoli N. Isoconversional kinetic analysis of thermally stimulated processes in polymers. Macromol Rapid Commun. 2006;27:1515–32.
32. Zhang J, Zeng JL, Liu YY, Sun LX. Thermal decomposition kinetics of the synthetic complex Pb(1,4-BDC)·(DMF)(H_2O). J Therm Anal Calorim. 2008;91:189–93.
33. Vyazovkin S. Model-free kinetics staying free of multiplying entities without necessity. J Therm Anal Calorim. 2006; 83:45–51.